Research Article

FATIGUE ANALYSIS ON A NEWLY DESIGNED HIP IMPLANTS WITH FINITE ELEMENT METHOD

Authors: Fatih Kaya, Gülhan İnce

To cite to this article: Kaya, F., İnce, G., FATIGUE ANALYSIS ON A NEWLY DESIGNED HIP IMPLANTS WITH FINITE ELEMENT METHOD, International Journal of Engineering and Innovative Research, 6(3), p 162-178.

DOI: 10.47933/ijeir.1540604

To link to this artice: https://dergipark.org.tr/tr/pub/ijeir/archive

International Journal of Engineering and Innovative Research

http://dergipark.gov.tr/ijeir

FATIGUE ANALYSIS ON A NEWLY DESIGNED HIP IMPLANTS WITH FINITE ELEMENT METHOD

Fatih Kaya[1], Gülhan İnce *[2]

[1]Burdur Mehmet Akif Ersoy University, Graduate School of Natural and Applied Sciences, Burdur, Turkey
[2] Department of Civil Engineering, Burdur Mehmet Akif Ersoy University, Turkey, 15030.

* Corresponding Author: gulhanince@mehmetakif.edu.tr
(**Received:** 30.08.2024; **Accepted:** 23.10.2024)

https://doi.org/10.47933/ijeir.1540604

ABSTRACT: This study used Finite Element Analysis (FEA) and Reverse Engineering (RE) methods to assess the fatigue performance of an originally designed cementless hip implant. The implant prototype was initially scanned using 3D scanning technology, and a finite element model was created. The implant was analyzed under dynamic loads for six different biomaterials commonly used, namely Ti-6Al-4V (Grade5), ASTM F3046 (Ti-3Al-2.5V), ASTM F75 (CoCr), ASTM F562(MP35N), ASTM F136(Ti6Al4V ELI), ASTM F67 (Ti Grade 4), and the fatigue life was evaluated. The results showed that the ASTM F75 (CoCr) implant had the highest stress and the ASTM F67 (Ti Grade 4) implant had the lowest stress. Also, Ti6Al4V (Grade 5) implant is performed better compared to fatigue than their counterparts made from ASTM F562(MP35N) and ASTM F67 (Ti Grade 4).

Keywords: Fatigue analysis, Dynamic loading, Finite element analysis, Implant.

1. INTRODUCTION

Hip arthroplasty was introduced in 1938 and is widely performed worldwide (0.3 million) each year *[1–3]*. More than two million Total Hip Replacements (THR) are performed annually worldwide. The number of surgeries has increased rapidly recently due to the increase in the elderly population *[4]*. According to the Canadian Joint Replacement Surgery report (2018-2019), the number of THR`s has increased by 20.1% in the last five years *[5]*. For example, in the last decade, 26% and 22% of revision surgeries were reported in Sweden *[6]* and the USA *[7]*, respectively. Osteoarthritis stands as one of the top ten debilitating afflictions in advanced nations. Globally, World Health Organization projections indicate a staggering 528 million individuals grappling with symptomatic osteoarthritis a startling surge of 113% since 1990 *[8]*.

While it is not possible to completely avoid hip implant problems, recent studies have shifted focus towards design tools that predict adverse situations more accurately. The design of hip implant necessitates collaboration between engineers and surgeons to ensure maximum stability and effectiveness [9]. In order to mitigate the destructive consequences of implant failure and anticipate such situations, various studies employing numerical methods aim to enhance the overall reliability of orthopedic implants. Advances in hip implant design, material properties, robotic surgical techniques, and experiences have significantly increased the lifetime of implants, making partial and total hip joint arthroplasty effective surgical treatments for managing arthritis [10]. However, instances of implant fatigue failure or loosening still persist [11–16]. Aseptic loosening of the implant often leads to implant failure.

The forces that human activity exerts on the hip implant generate dynamic stresses that change over time and lead to dynamic failure of the implant. Consequently, it is important to ensure implant resistance to dynamic failure [4].

S-N data, also known as stress-life or fatigue data, represents the relationship between the applied stress (S) and the number of cycles to failure (N) for a material or component subjected to cyclic loading. This data is crucial for predicting the fatigue life of engineering materials and structures.

In S-N data, the stress amplitude (S) is plotted on the x-axis, usually using a logarithmic scale, while the number of cycles to failure (N) is plotted on the y-axis. The data is typically obtained through experimental testing, where specimens are subjected to cyclic loading at different stress levels until failure occurs. The number of cycles to failure for each stress level is recorded, and this data is then plotted to create an S-N curve. The S-N curve provides valuable information about the fatigue behavior of a material or component, including its fatigue strength, endurance limit, and fatigue life under specific loading conditions. Engineers use S-N data to design components and structures that can withstand cyclic loading without failure, by ensuring that the applied stresses remain below the fatigue limit predicted by the S-N curve. Additionally, S-N data can be used to evaluate the effect of different factors such as material properties, surface finish, environmental conditions, and loading frequency on fatigue performance. This information is essential for optimizing designs and selecting appropriate materials to enhance the fatigue resistance of engineering components and structures [17].

Fatigue is an important design criterion to ensure that implant have a sufficiently high level of safety. Standard fatigue tests can estimate the fatigue service life of materials, but experimental methods are too expensive and take a long time for material selection or optimization. It may be necessary to retest for a slightly different situation, whereas the experiment has already been performed. There are a number of comparative studies between fatigue life simulation analysis and experimental fatigue results, showed that a well- configured Finite Element Analysis (FEA) can correctly indicate the actual stress variations of the hip implant [18–22]. In circumstances were overcoming complicated engineering problems, the FEA has proven to be a powerful and dependable numerical method for analyzing structures subjected to various types of loads. It is well known that a finite element solution is always a near solution to the relevant real-world problem and one always must decide whether it is a good or a bad solution. In response, ASTM International recently announced the F2996-20 [23] standard, which offers a reliable FEA procedure for examining hip stems used in hip implant surgery. This standard has been established for guidance to implant designers via the process of FEA for hip implants according to ISO 7206-4 [24] and ISO 7206-6 [25] standards.

From the search of open literature, although there are many fatigue FEA studies on hip implant with various loading types and boundary conditions, fewer studies have reported accordance with ISO 7206-4 [24] and ASTM F2996-20 [23] loads and boundary conditions [9, 26–30]. The publications [11, 18, 26, 31–33] are also studied fatigue failure analysis of various materials and geometrical design at different loading patterns. Pianigiani and Alemani [34] have studied to what degree of the test parameters can affect the outputs under ISO 7206-4 [24] boundary conditions. They determined that potential ranges of acceptance limits for the validation of numerical models repeating the boundary conditions. Simoneau et al. [35] considered only static FEA, and its experimental validation of porous Ti6Al4V metallic femoral stem produced with selective laser melting. Triyono et al. [36] have investigated element size variation effect

on mechanical behavior of hip stem implant design using FEA method. This method was also employed to determine the cause of implant failure as well as chemical analysis by energy-dispersive spectroscopy, optical microscopy, scanning electron microscopy, image processing techniques, etc. [37].

In this study, the fatigue life of a newly designed hip implant subjected to cyclic loading was investigated through reverse engineering and finite element analysis. The obtained results have been compared with those of commonly used implant alloys. The cyclic loading pattern is defined according to ISO 7206-4 [24] and ISO 7206-6 [25]. A numerical three-dimensional (3D) finite element model of the hip implant was developed based on the mechanical properties and fatigue characteristics specified in the material certificate, along with experimental fatigue S-N curve data.

2. METHODOLOGY

2.1. Examined Implant

The prototype implant presented in this study is a newly designed non-modular uncemented long-stem hip implant designed with a rectangular cross-section and rounded corners. Also, oriented asymmetrical grooves are located in the proximal medial region of the femur (Figure 1). Its purpose is to transmit the principal stress applied to the bone within the grooves, which is an important factor for maximum principal stress distribution. The implant stem is a cold-forged Ti–6Al–4V (Grade 4) titanium alloy. It has a rough grit basted surface. Hip implant stem was hydroxyapatite-coated to improve anatomically ingrown. Surface modification techniques have been developed significantly in the last couple of decades for enhanced tribological performance of hip implant. Surface modification techniques improve biological, chemical and mechanical properties of implant surfaces. A new surface modification was created to obtain bone function suitable for the microstructure of the implant.

Figure 1. Newly designed cementless long-stem hip implant prototype and its asymmetric groove designs

Table 1 and 2 summarizes the mechanical and chemical properties of the Ti6Al4V (Grade 4) titanium alloy material used in the production of the hip implant prototype, which is derived from the mill test certificate.

Table 1. Mechanical properties of the prototype implant material

Material	Young Modulus	Poisson's ratio	Yield strength	Ultimate tensile strength
Ti6Al4V Grade 5 [38]	114000 MPa	0.34	1089MPa	1182MPa
ASTM F3046 (Ti-3Al-2.5V)[38]	105000 MPa	0.34	485MPa	685MPa
ASTM F75 (CoCr)[39]	220000 MPa	0.30	450MPa	665MPa
ASTM F562 (MP35N)[40]	243150 MPa	0.29	1813MPa	1882MPa
ASTM F136 (Ti6Al4V ELI)[38]	117000 MPa	0.32	961MPa	1036MPa
ASTM F67 (Grade 4)[38]	120000 MPa	0.36	669MPa	738MPa

Table 2. Chemical composition of Ti6Al4V (Grade 4) (%)

Position	Ti	Fe	C	N	H	O	Al	V	Other
Top	Remainder	0.05	0.01	0.01	0.001	0.08	5.90	4.00	Each<0.10
Middle	Remainder	0.05	0.01	0.01	0.001	0.08	5.90	4.00	Total<0.40

2.2. 3D Scanning and Modelling

3D scanning technology is often used in biomedical engineering and it is an accurate method of recreating implant geometry. The hip implant prototype was converted to a Computer Aided Design (CAD) model using Three-Dimensional (3D) scanning technology. In this study, NextEngine® 3D Ultra High Definition (HD) Desktop laser scanner was used for scanning. NextEngine® Ultra HD is laser-based tracing scanner presents a high resolution of 0.125 mm. It is able to scan 50 000 spots per second with high precision. However, if scanning data is incorrectly positioned, aligned, or integrated, can be led to unwanted results. NextEngine® 3D scanner and scanning setup are shown in Figure 2.

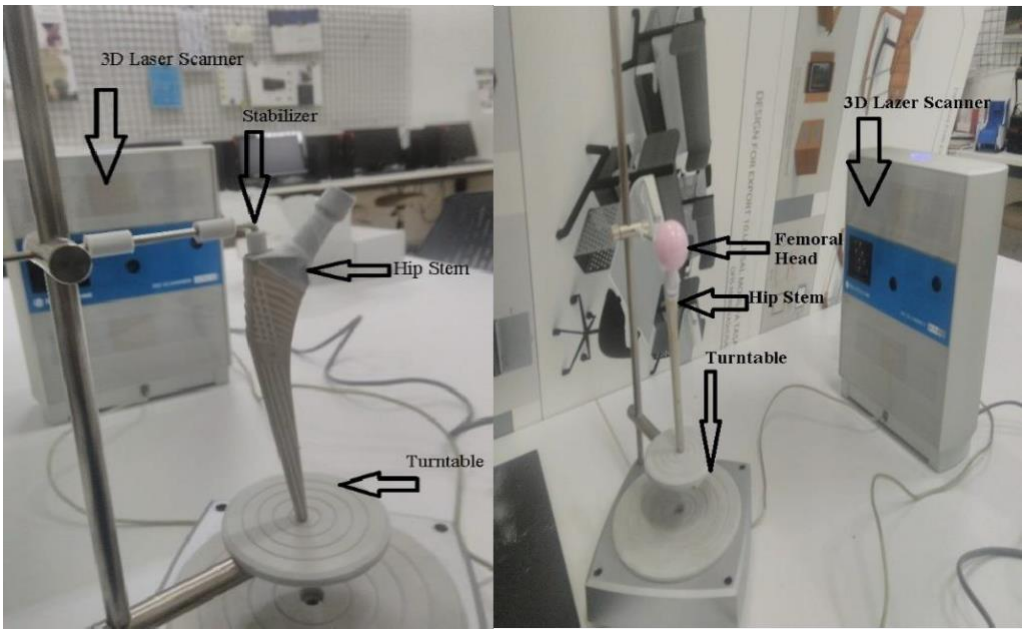

Figure 2. Nextengine 3D laser scanner and scanning setup

By using the Sampling Method within the Geomagic for Solidworks extension in Solidworks 2017 software, the sample data was reduced to 33% and grid sample points were selected as 1/4, reducing the number of point clouds to a reasonable size (545,370). In this way, the surface and solid model was obtained successfully from the scanning data.

With the deviation analysis tool included in the Geomagic for SOLIDWORKS 2017 extension, 3D deviation analysis was performed to check the quality and accuracy of 3D scanning. The 3D CAD model was compared with the original scanning data, and the deviation amount of the model was checked. The 3D CAD model and the deviation analysis results are shown in Figure 3.

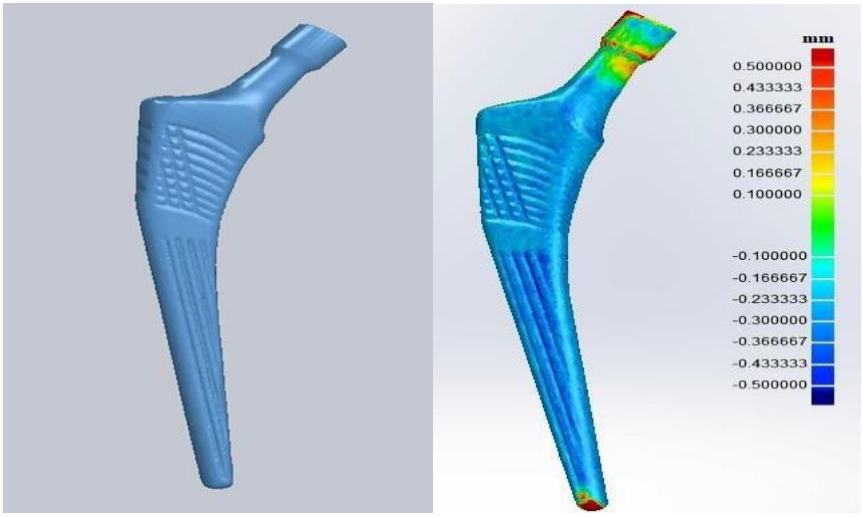

Figure 3. 3D CAD model and deviation analysis result by compared with CAD data and scanning data

2.3. Finite element modeling

2.3.1. Meshing

The FE model was created through Ansys Workbench commercial software 2019 R1 [41]. The neck region, the driver hole, and the potting regions on the implant are critical areas where the stress and strain values are high. This model was meshed with three-dimensional tetrahedron elements. Achieving mesh independence ensures that the FEA solution converges to a consistent outcome. Proper meshing and achieving mesh independence are critical steps to obtain reliable resultsa [42]. The Adaptive Mesh Convergence method was used to achieve mesh-independent results. It helps obtain solutions that are independent of the mesh, ensuring that the results do not change noticeably with further mesh refinement. This approach can assist in defining better mesh controls for future models, ensuring numerical accuracy. Mesh convergence criteria have been set at 5% according to the ASTM F2996-20[26] resulting in a total number of elements and nodes of 219,587 and 312,443 respectively. Inherently, this type of element consists of ten nodes per element. The body of FE model shown in Figure 4. A smooth and sufficiently dense finite element mesh is essential for accurately calculating local stresses in fatigue analysis.

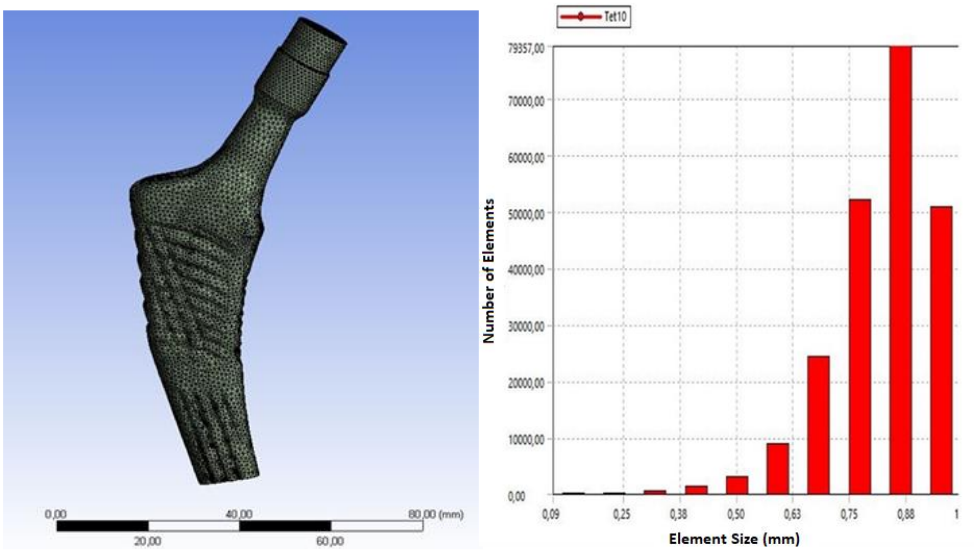

Figure 4. Finite element mesh structure and element size distribution of the prototype model

2.3.2. Loading and boundary conditions

In literature, static FEA are generally performed using various bodyweight loads *[43–45]*. However, the effects of rapid movement can increase the load of body weight. Therefore, it is necessary to analyze the implant under static loads corresponding to the specified in ISO 7206-4 *[24]* loads *[43]*. ASTM F2296-20, ISO 7206-4 and ISO 7206-6 outlines important boundary and loading conditions for static and fatigue testing of orthopedic implants, particularly hip joint prostheses. Key boundary conditions include secure fixation of the implant at specific points to prevent movement, along with a rigid support structure that simulates the surrounding bone. Loading conditions require the applied design load (FD) reflecting the maximum expected load during daily activities. Additionally, the angle of load application is crucial for affecting stress distribution and potential failure modes, and the testing must include cyclic loading to simulate repetitive human activity, typically up to 5.000.000 cycles. In this study, FE static and fatigue analysis was performed considering the loading and boundary conditions status given in ASTM F2296- 20 *[23]*, ISO 7206-4 *[24]* and ISO 7206-6 *[25]* standards. By adhering to ASTM F2996-20 standards and accurately replicating loading and boundary conditions relevant to real-world scenarios, engineers can ensure that the performance and durability of hip implants are rigorously evaluated, ultimately leading to safer and more effective medical devices for patients. According to ASTM F2996-20 “worst-case scenario”, hip implant model loaded vertically with max. 2300 N and min. 50 N. Displacements and rotations constrained at the potting level with fixed support boundary conditions were implemented. Applied boundary conditions are shown in Figures 5-6. The load and boundary conditions are stated as follows:

- D =80mm
- F_D =2300 N
- $\alpha = 10° \pm 1°$
- $\beta = 9° \pm 1°$

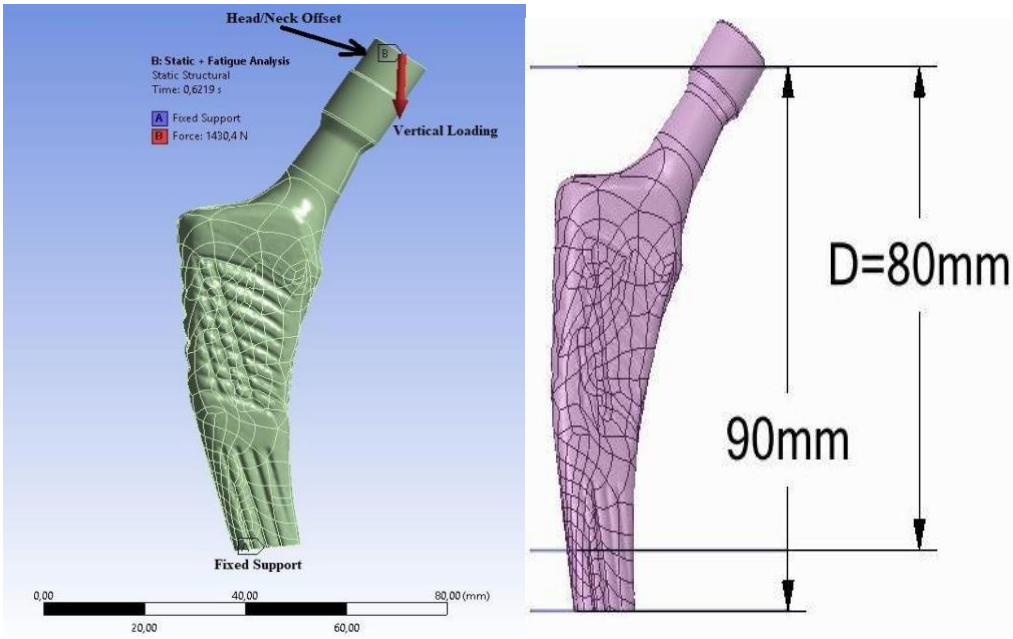

Figure 5. Loading and embedding depth of the prototype model

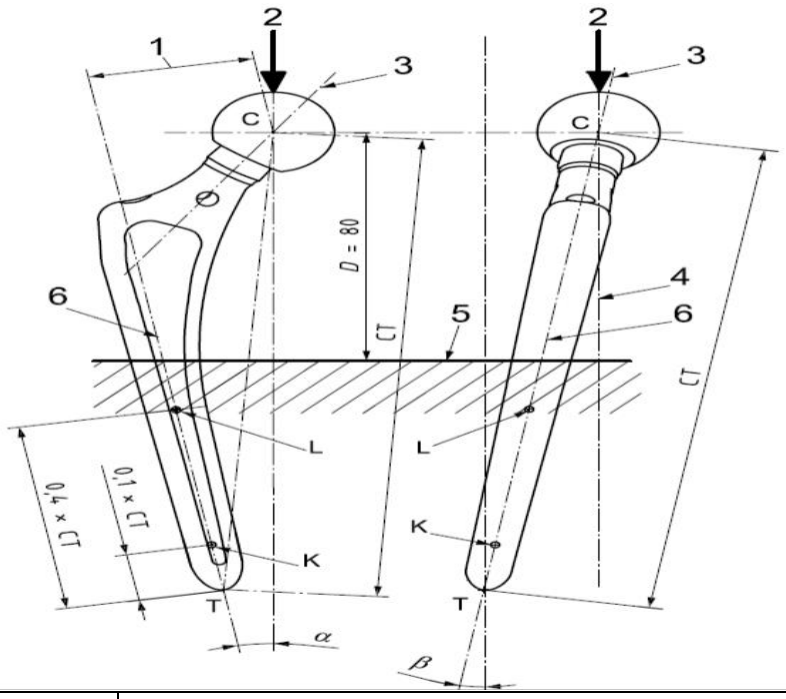

1 Head offset	T most distal point of stem
2 Load point	C center of head
3 Neck axis	D potting level
4 Load axis	K, L points at specific distance from T, which define the stem axis
5 Cement level	α angle in the frontal plane CKL between the load axis 4 and the stem axis 6
6 Stem axis KL	β angle in the lateral plane perpendicular to CKL between the load axis 4 and the stem axis 6

Figure 6. Positioning the test specimen under test for symmetrical stems with CT distance 120 mm < CT ≤ 250 mm [24]

The distal axis is positioned to be directed at an angle α and the proximal axis at an angle β (Figure 7). D is the distance from the center of the femoral head to the level of potting. For fatigue FE analysis, the design load FD shown in Table 3 was performed according to the rules and procedures described in ISO 7206-4 [24] until the 5.000.000 cycle without the occurrence of failure.

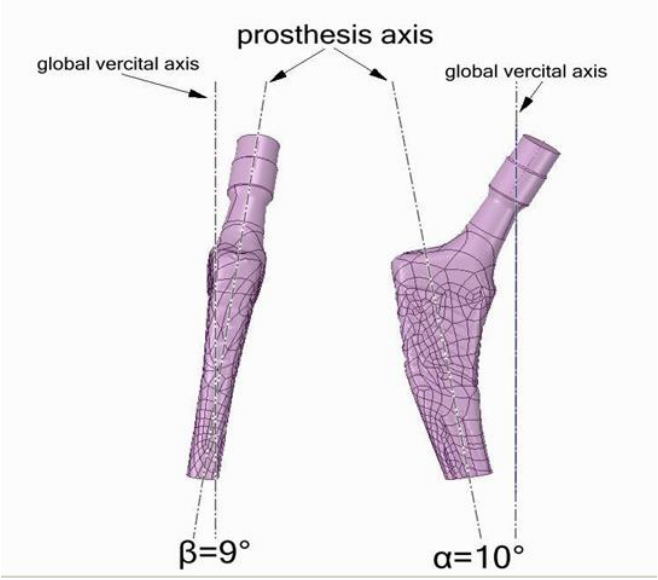

Figure 7. Femoral stem α (right) and β(left) orientation according to ISO 7206-4 [24]

Table 3. Strength performance parameters according to ISO 7206-4 [24]

Type of Femoral stem	Short, monoblok, modular neck, modular femur		
CT (mm)	≤120	120<CT≤250	>250
FD (N)	1200a	2300b	1200[c]
Number of Cycle	$5x10^6$		

2.4. Fatigue FE Analysis of Implant

Fatigue life of the implant is estimated with FEA using ANSYS. To obtain the fatigue life, the S-N curve is an important parameter showing the relationship between alternating stress and number of cycles. The S-N curve for Ti6Al4V is shown in Figure 8.

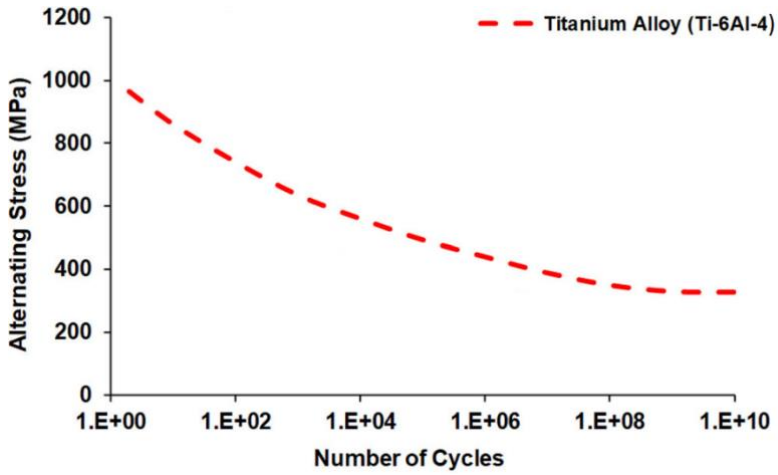

Figure. 8 The alternating stress versus the number of cycles (S-N graphs) [46]

Goodman, Soderberg, and Gerber theories are commonly used in engineering to account for the mean stress effect in fatigue analysis. Selecting these theories depends on the specific characteristics of the loading conditions and the material properties involved. By considering factors such as the magnitude and distribution of stress, engineers can choose the most appropriate theory to accurately predict fatigue failure in the given application. In general, most experimental data fall. The Goodman theory can be a good choice for brittle materials with the Gerber theory usually a good choice for ductile materials The Gerber theory treats negative and positive mean stresses equally, while Goodman and Soderberg criteria are not limited when considering negative mean stresses. Consequently, within the ANSYS fatigue module, alternating stresses are capped by disregarding the negative mean stress.

In this study Goodman, Soderberg, and Gerber's theories used to calculation of the mean stress effect on fatigue life. Generalized formulations [4, 47] are expressed as following, respectively

$$\left(\frac{\sigma_a}{S_e}\right) + \left(\frac{\sigma_m}{S_u}\right) = \frac{1}{N_s} \tag{1}$$

$$\left(\frac{\sigma_a}{S_e}\right) + \left(\frac{\sigma_m}{S_y}\right) = \frac{1}{N} \tag{2}$$

$$\left(\frac{N\sigma_a}{S_e}\right) + \left(\frac{N\sigma_m}{S_u}\right)^2 = 1 \tag{3}$$

Where S_y, N_s, S_e and S_u are material's yield stress, fatigue safety factor, endurance limit and ultimate tensile strength of the material respectively. Mean stresses calculated based on Von-Mises stresses. Alternating stress is defined as following:

$$\sigma_a = \frac{(\sigma_{\max} - \sigma_{\min})}{2} \tag{4}$$

ISO 7206-4 [24] established a test procedure to determine the strength characteristics of the total hip joint and neck region of stemmed femoral components used solely in the partial hip joint. In addition, defines the testing conditions that consider important parameters affecting the components.

According to ISO 7206-4 [24], hip stem fatigue test loading conditions should be sinusoidal loading and the value of the minimum load in the load cycle necessary to be a force between 500 N and 600 N. In this study, the sinusoidal type cycling loading applied vertically.

Frequency is ignored due to considering time-domain (stress-life) fatigue analysis. R-ratio stress curves are similar to the mean value stress curves. The present FEA employs boundary and loading conditions following the ASTM F2996-13 and ISO 7206-4:2010(E) standards, respectively. Owing to computational constraints, dynamic, torsional, and tensile forces are excluded from consideration in this study. All materials undergo analysis under a maximum 2300N force applied at the proximal end of the stem, while the areas of the distal end remain fixed to finalize the analysis. The ANSYS FEA is utilized to examine the homogeneous model with various materials. Instead of maintaining a particular mean stress, a consistent loading ratio was applied. The minimum and maximum loads are applied as 500N and 2300 N (load ratio: 0.2174), respectively.

3. NUMERICAL RESULTS AND DISCUSSION

3.1. Evaluation of Static Analysis Results

Linear static FE analysis was performed based on the instructions presented in ISO 7206-4 [24] and ASTM F2996-20 [23] standards. Maximum principal stress, and strain results are shown in Figure 9 and Table 4.

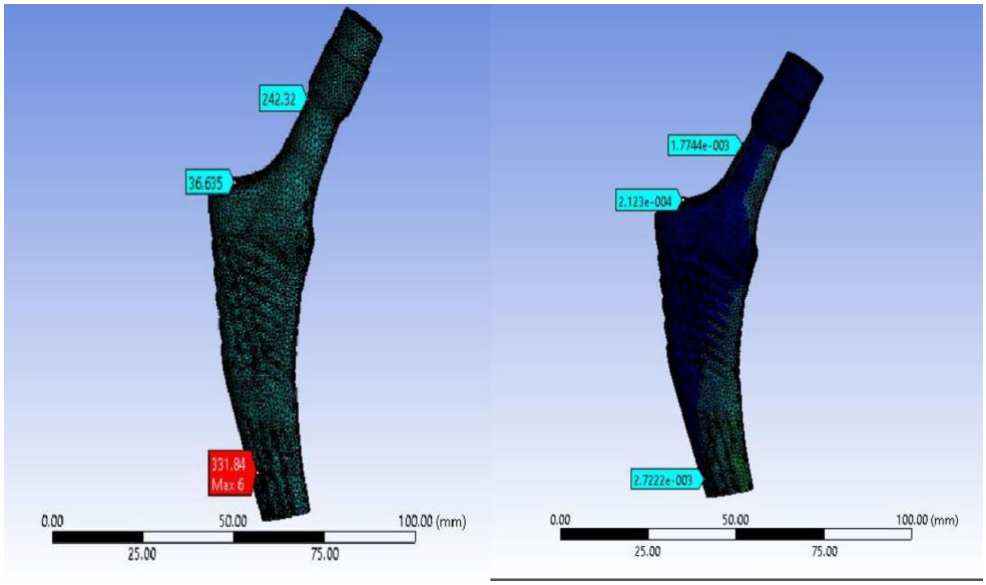

Figure 9. Maximum principal stresses(left) and strains(right) of the prototype model

Table 4. Static structural stress and strain results of the prototype model

Results Type	Neck Region	Driver Hole	Potting Level
Maximum Principal Stress (MPa)	242.32	36.635	331.84
Von-Mises Stress (MPa)	298.02	36.413	345.03
Strain(mm/mm)	0.00203	0.0009	0.00316

For the newly designed hip implant prototype presented in this study, the highest stress occurred in the potting level of 331.8 MPa, while the smallest stress occurred in the driver hole 36.6 MPa. The value of the stress in the neck area is 242.3 MPa. Compared to the studies in the literature, according to the result given in ASTM F2296-20 [23], while the stresses in the neck region and driver hole lower, the stress in the potting level is upper. According to the result of Wimalasiri [48], while the tension in the neck region is upper, the tension in the potting level is lower and acceptable level. According to the study results of Munteanu et al. [49] and optimized Munteanu et al. [49], the stress lower both at the fixation zone. A comparison of stress levels in the present study with reported literature is shown in Table 5.

Table 5. Comparison of stress levels and maximum stress regions

Maximum Principal Stress Regions	Neck Region (MPa)	Driver Hole (MPa)	Potting Level (MPa)
Present Study	242.3	36.6	331.8
Wimalasiri [48]	175	-	1321
ASTM F2296-20 (Average of seven studies)	411.61	179.2	166.1
Munteanu et al. [49]	-	-	478.6
Optimized Munteanu et al. [49]	-	-	349.1

Presented FE model results were compared to previously published five different studies obtained from the search of open literature. All five implant has different geometrical shapes and cross-section areas in various regions (Figure 10). Moreover, while the present study, Wimalasiri [48] and ASTM F2296-20 [23] made from Ti-6A1-4V, Munteanu et al. [49] and optimized Munteanu et al. [49] manufactured Ti6Al4V powder by powder bed fusion (PBF) technic. Manufacturing techniques have a significant effect on the static and fatigue performance of hip implant material [32, 37, 47, 50, 51]. Therefore, all implants can have different stress and fatigue strength at the same loading and boundary conditions depending on the material's fatigue properties, production process and implant geometry.

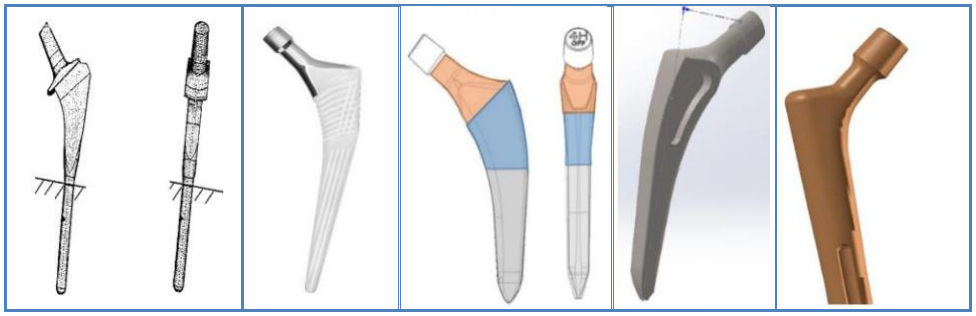

(a) (b) (c) (d) (e)

Figure 10. Hip implant models: Wimalasiri [48] (a) present study (b), Munteanu et al.[49] (c), optimized Munteanu et al. [49](d), ASTM F2296-20 [23]

3.2. Evaluation of Fatigue Analysis Results

High-cycle stress-life fatigue FE analysis was conducted based on ISO 7206-4 standard conditions. Stress analysis neglected bone cement stresses and applied sinusoidal-type cyclic loading vertically. The hip implant FE model aimed to withstand ISO 7206-4 conditions for $5x10^6$ cycles without failure. Equivalent stresses were determined using Von-Mises yield criterion, and various mean stress theories were applied in fatigue analysis. The equivalent alternating stresses obtained from the FEA are shown in Table 6 and Figs. 11-12. Fatigue stress results from this study align well with common Ti-6Al-4V implant alloys.

Table 6. Finite elements equivalent stresses of the prototype model (Ti6Al4V)

Mean Stress Theory	Maximum Equivalent Alternating Stress
Goodman (MPa)	530.76
Soderberg (MPa)	536.38
Gerber (MPa)	531.76
Mean Stress Curves (MPa)	530.76

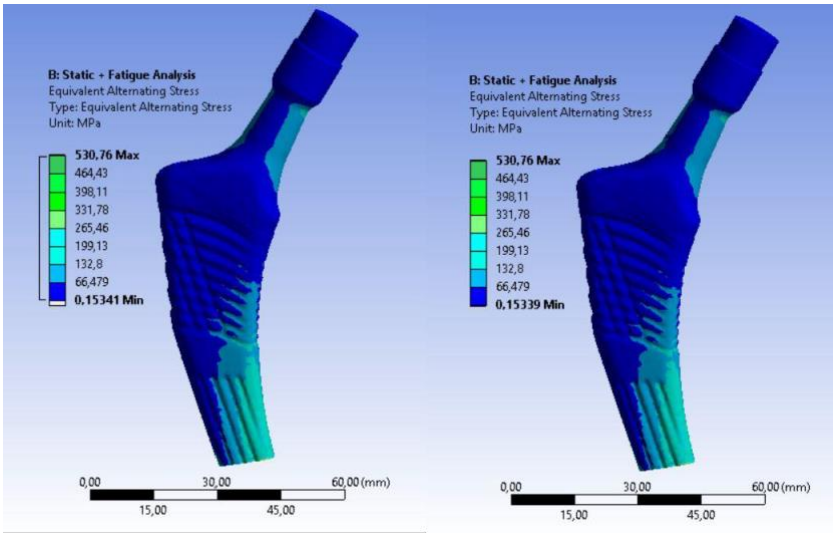

Figure 11. Equivalent alternating stresses: Goodman (left) and mean stress (right)

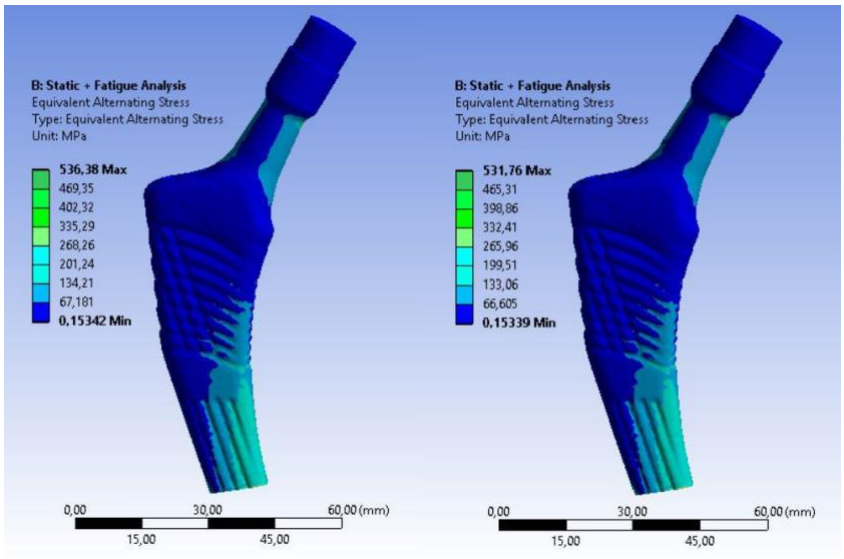

Figure 12. Equivalent alternating stresses: Soderberg (left) and Gerber (right)

To understand the effects of different materials on fatigue behavior on the same geometry, six different implant materials were assigned to the FEA model. The fatigue stress results of all studied materials are shown in Figure 13.

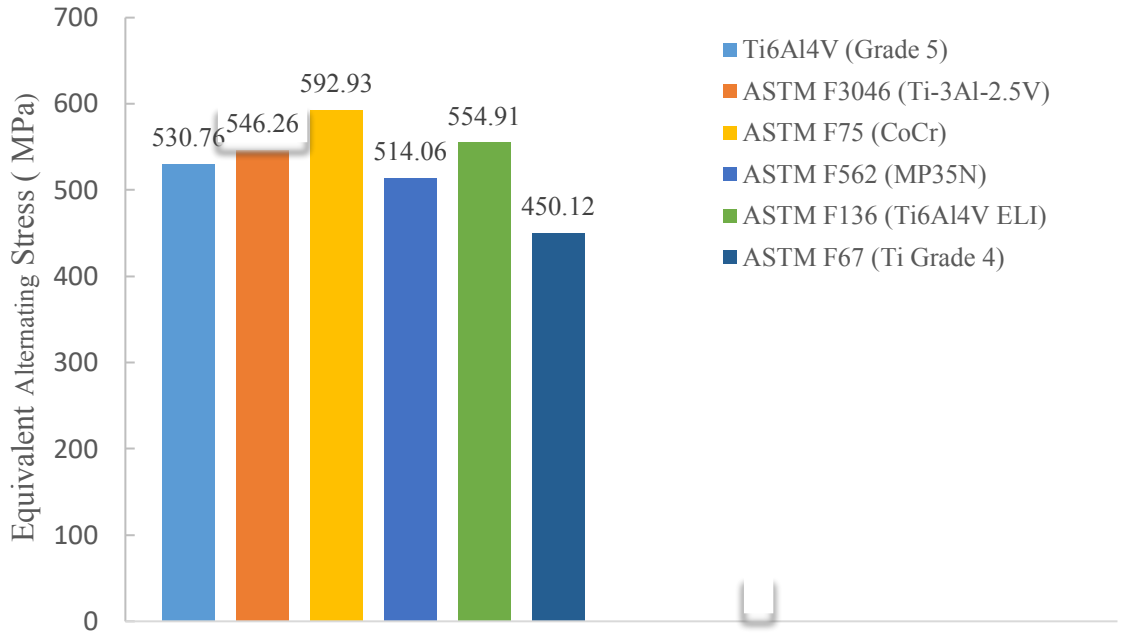

Figure 13. Finite element fatigue simulation results of some common hip implant materials for proposed stem geometry

Considering the implant prototype as a cantilever, it can be considered an isostatic system as a bar. While changing material parameters affects fatigue alternating stresses, it also causes a change in strain distribution and displacement. However, the finite 3D elements used here, beyond the bar assumption, result in limited changes in stresses. Fatigue simulation results of this study were compared with previous experimental and numerical fatigue results based on ISO 7206-4 [24] and 7206-6 [25] loads and boundary conditions, as shown in Table 7.

Table 7. Comparison of finite elements equivalent fatigue stress results

Study	Material	Equivalent Stress (MPa)	Maximum Stress Region
Delikanli and Kayacan [52]	Ti6Al4V alloy metal powder	211.5	Neck Region
Ploeg et al. [20]	Ti6Al4V ELI	352	Potting Level
He et al. [53]	Ti-6Al-4V	575	Unspecified
Present Study	Ti-6Al-4V (Grade5)	530.76	Neck Region
Present Study	ASTM F3046 (Ti-3Al-2.5V)	546.26	Neck Region
Present Study	ASTM F75 (CoCr)	592.93	Neck Region
Present Study	ASTM F562(MP35N)	514.06	Neck Region
Present Study	ASTM F136 (Ti6Al4V ELI)	554.91	Neck Region
Present Study	ASTM F67 (Ti Grade 4)	450.12	Neck Region

The fatigue analysis of the newly designed hip implant prototype revealed the highest maximum stress at 592.93 MPa on the neck region of ASTM F75 CoCr Alloy. The lowest maximum stress was found at 450.12 MPa on the neck region of ASTM F67 Titanium Alloy. The results obtained are in agreement with the literature [28, 53–55]. The Ti6Al4V (Grade 5) titanium

prototype has lower stress than their counterparts made of ASTM F75 (CoCr), ASTM F136 (Ti6Al4V ELI) and ASTM 3046 (Ti-3Al-2.5V).

Compared to literature values, the newly designed prototype implant in the study decreased tension in the neck area and the driver hole, while tensions in the region of the potting level increased. The design appears safe, considering that high stresses mostly occur at the neck and potting levels. Hosseini et al. [56] gave a limit value for Ti-6Al-4V implant alloys in his study is 555 MPa. Accordingly, the maximum stresses obtained for Ti-6Al-4V remained below the limit given by Hosseini et al.[56]. Also, the maximum stress obtained for the implant prototype in this study is lower than the stress obtained in He et al. [53] for the Ti-6Al-4V material.

4. CONCLUSIONS

The aim of this study was to evaluate the fatigue performance of a newly designed cementless hip implant by finite element analysis and to contribute the enhancement of knowledge in this research field. In the study, a total of six implant finite element models with different materials, including one newly designed Ti6Al4V (Grade 5) implant prototype, were analyzed and the results were evaluated. The results obtained from the analysis are summarized as follows:

The mean stress of the newly designed Ti6Al4V (Grade 5) implant was found to be below the limit value, indicating its safety against fatigue failure. This suggests that the material and design of the newly designed implant meets the required mechanical specifications.

The highest stress was obtained in the ASTM F75 (CoCr) implant and the lowest in the ASTM F67 (Ti Grade 4) implant. Evaluation of fatigue life revealed that Ti6Al4V (Grade 5) performed better compared to ASTM F562 (MP35N) and ASTM F67 (Ti Grade 4).

The results provide insights into how different materials perform under loading conditions, guiding material selection for future designs.

Acknowledgments

The authors would like to thank Ortonom Medikal Ltd. Company for providing the implant.

REFERENCES

[1] Rubak, T. S., Svendsen, S. W., Søballe, K., & Frost, P. (2014). Total Hip Replacement due to Primary Osteoarthritis in Relation to Cumulative Occupational Exposures and Lifestyle Factors: A Nationwide Nested Case–Control Study. *Arthritis Care & Research*, *66*(10), 1496–1505. https://doi.org/10.1002/acr.22326

[2] Dopico-González, C., New, A. M., & Browne, M. (2010). Probabilistic finite element analysis of the uncemented hip replacement—effect of femur characteristics and implant design geometry. *Journal of Biomechanics*, *43*(3), 512–520. https://doi.org/10.1016/j.jbiomech.2009.09.039

[3] Ebramzadeh, E., Normand, P. L., Sangiorgio, S. N., Llinás, A., Gruen, T. A., McKellop, H. A., & Sarmiento, A. (2003). Long-term radiographic changes in cemented total hip arthroplasty with six designs of femoral components. *Biomaterials*, *24*(19), 3351–3363. https://doi.org/10.1016/S0142-9612(03)00187-X

[4] Joshi, T., Sharma, R., Mittal, V. K., Gupta, V., & Krishan, G. (2022). Dynamic fatigue behavior of hip joint under patient specific loadings. *International Journal of Automotive and Mechanical Engineering*, *19*(3), 10014–10027. https://doi.org/10.15282/ijame.19.3.2022.13.0773

[5] CIHI. (2022). *Hip and Knee Replacements in Canada: CJRR Annual Report, 2020–2021 — Updated September 2022*. Canadian Institute for Health Information.

[6] Kärrholm, J., Rogmark, C., Nauclér, E., Nåtman, J., Vinblad, J., Mohaddes, M., & Rolfson, O. (2019). *Swedish Hip Arthroplasty Register*. Department of Orthopaedics, Sahlgrenska University Hospital.
[7] Bozic, K. J., Kurtz, S. M., Lau, E., Ong, K., Vail, T. P., & Berry, D. J. (2009). The epidemiology of revision total hip arthroplasty in the United States. *The Journal of Bone and Joint Surgery. American Volume*, *91*(1), 128–133. https://doi.org/10.2106/JBJS.H.00155
[8] OECD. (2023). *Health at a Glance 2023: OECD Indicators*. Paris: Organisation for Economic Co-operation and Development. Retrieved from https://www.oecd-ilibrary.org/social-issues-migration-health/health-at-a-glance-2023_7a7afb35-en
[9] Woiczinski, M., Maas, A., Grupp, T., Thorwächter, C., Santos, I., Müller, P. E., … Steinbrück, A. (2020). Realitätsnahe Finite-Elemente-Simulation in der präklinischen Testung von Knie- und Hüftimplantaten. *Der Orthopäde*, *49*(12), 1060–1065. https://doi.org/10.1007/s00132-020-04025-0
[10] Marsh, M., & Newman, S. (2021). Trends and developments in hip and knee arthroplasty technology. *Journal of Rehabilitation and Assistive Technologies Engineering*, *8*, 2055668320952043. https://doi.org/10.1177/2055668320952043
[11] Griza, S., Kwietniewski, C., Tarnowski, G. A., Bertoni, F., Reboh, Y., Strohaecker, T. R., & Baumvol, I. J. R. (2008). Fatigue failure analysis of a specific total hip prosthesis stem design. *International Journal of Fatigue*, *30*(8), 1325–1332. https://doi.org/10.1016/j.ijfatigue.2007.11.005
[12] Eachempati, K. K., Dannana, C. S., Apsingi, S., Ponnala, V. K., Boyapati, G., & Parameswaran, A. (2020). Trunnion fracture of femoral prosthesis following a large metal-on-metal uncemented total hip arthroplasty: a case report. *Arthroplasty (London, England)*, *2*(1), 32. https://doi.org/10.1186/s42836-020-00055-3
[13] Grupp, T. M., Weik, T., Bloemer, W., & Knaebel, H.-P. (2010). Modular titanium alloy neck adapter failures in hip replacement-failure mode analysis and influence of implant material. *BMC musculoskeletal disorders*, *11*, 3. https://doi.org/10.1186/1471-2474-11-3
[14] Janssen, D., Aquarius, R., Stolk, J., & Verdonschot, N. (2005). Finite-element analysis of failure of the Capital Hip designs. *The Journal of Bone & Joint Surgery British Volume*, *87-B*(11), 1561–1567. https://doi.org/10.1302/0301-620X.87B11.16358
[15] Łapaj, Ł., Woźniak, W., Wiśniewski, T., Rozwalka, J., Paczesny, Ł., Zabrzyński, J., … Kruczyński, J. (2019). Breakage of metal hip arthroplasty components: Retrieval and structural analysis. *Bio-Medical Materials and Engineering*, *30*(3), 297–308. https://doi.org/10.3233/BME-191053
[16] Mierzejewska, Ż. A. (2015). Case Study and Failure Analysis of a total hip Stem Fracture. *Advances in Materials Science*, *15*(2), 5–13.
[17] Fouchereau, R., Celeux, G., & Pamphile, P. (2014). Probabilistic modeling of *S–N* curves. *International Journal of Fatigue*, *68*, 217–223. https://doi.org/10.1016/j.ijfatigue.2014.04.015
[18] Pekedis, M., & Yildiz, H. (2011). Comparison of fatigue behaviour of eight different hip stems: a numerical and experimental study. *Journal of Biomedical Science and Engineering*, *4*(10), 643–650. https://doi.org/10.4236/jbise.2011.410080
[19] Şik, A., Önder, M., & Korkmaz, M. S. (2015). Taşit jantlarinin yapisal analiz ile yorulma dayaniminin belirlenmesi. *Gazi University Journal of Science Part C: Design and Technology*, *3*(3), 565–574.
[20] Ploeg, H.-L., Bürgi, M., & Wyss, U. P. (2009). Hip stem fatigue test prediction. *International Journal of Fatigue*, *31*(5), 894–905. https://doi.org/10.1016/j.ijfatigue.2008.10.005
[21] Zameer, S., & Haneef, M. (2015). Fatigue life estimation of artificial hip joint model using finite element method. *Materials Today: Proceedings*, *2*(4), 2137–2145. https://doi.org/10.1016/j.matpr.2015.07.220
[22] Cadario, A., & Alfredsson, B. (2007). Fatigue growth of short cracks in Ti-17: Experiments and simulations. *Engineering Fracture Mechanics*, *74*(15), 2293–2310. https://doi.org/10.1016/j.engfracmech.2006.11.016
[23] ASTM F2996-20. (2020). Standard Practice for Finite Element Analysis (FEA) of Non-Modular Metallic Orthopaedic Hip Femoral Stems. PA, USA. Retrieved from https://www.astm.org/f2996-20.html
[24] ISO 7206-4:2010. (2010). Implants for surgery - Partial and total hip joint prostheses - Part 4: Determination of endurance properties and performance of stemmed femoral components. Geneva, Switzerland. Retrieved from https://www.iso.org/standard/42769.html
[25] ISO 7206-6:2013. (2013). Implants for surgery - Partial and total hip joint prostheses - Part 6: Endurance properties testing and performance requirements of neck region of stemmed femoral components. Geneva, Switzerland. Retrieved from https://www.iso.org/standard/51186.html
[26] Senalp, A. Z., Kayabasi, O., & Kurtaran, H. (2007). Static, dynamic and fatigue behavior of newly designed stem shapes for hip prosthesis using finite element analysis. *Materials & Design*, *28*(5), 1577–1583. https://doi.org/10.1016/j.matdes.2006.02.015
[27] Carbone, V., Palazzin, A., Bisotti, M. A., Bursi, R., & Emili, L. (2020). An integrated cloud platform to perform in silico standard testing for orthopaedic devices. *Orthopaedic Proceedings*, *102-B*(SUPP_11), 2–2. https://doi.org/10.1302/1358-992X.2020.11.002
[28] Joshi, T., & Gupta, G. (2021). Effect of dynamic loading on hip implant using finite element method. *Materials Today: Proceedings*, *46*, 10211–10216. https://doi.org/10.1016/j.matpr.2020.11.378

[29] Chethan, K. N., Zuber, M., Bhat N, S., & Shenoy B, S. (2020). Optimized trapezoidal-shaped hip implant for total hip arthroplasty using finite element analysis. *Cogent Engineering*, *7*(1), 1719575. https://doi.org/10.1080/23311916.2020.1719575
[30] Babić, M., Verić, O., Božić, Ž., & Sušić, A. (2020). Finite element modelling and fatigue life assessment of a cemented total hip prosthesis based on 3D scanning. *Engineering Failure Analysis*, *113*, 104536. https://doi.org/10.1016/j.engfailanal.2020.104536
[31] Knight, S. R., Aujla, R., & Biswas, S. P. (2011). Total Hip Arthroplasty - over 100 years of operative history. *Orthopedic Reviews*, *3*(2), e16. https://doi.org/10.4081/or.2011.e16
[32] Desai, C., Hirani, H., & Chawla, A. (2015). Life Estimation of Hip Joint Prosthesis. *Journal of The Institution of Engineers (India): Series C*, *96*(3), 261–267. https://doi.org/10.1007/s40032-014-0159-4
[33] Abdullah, K. (2010). Study of Factors Affecting Taper Joint Failures in Modular Hip Implant Using Finite Element Modelling. In *Modeling Simulation and Optimization - Focus on Applications*. IntechOpen. https://doi.org/10.5772/8973
[34] Pianigiani, S., & Alemani, F. (2020). Evaluating the effects of experimental settings during iso 7206-4 endurance and performace tests: a finite element analysis. *Journal of Mechanics in Medicine and Biology*, *20*, 1–13. https://doi.org/10.1142/S0219519420500062
[35] Simoneau, C., Terriault, P., Jetté, B., Dumas, M., & Brailovski, V. (2017). Development of a porous metallic femoral stem: Design, manufacturing, simulation and mechanical testing. *Materials & Design*, *114*, 546–556. https://doi.org/10.1016/j.matdes.2016.10.064
[36] Ikhsan, J., Prabowo, A. R., & Sohn, J. M. (2020). Investigation of meshing strategy on mechanical behaviour of hip stem implant design using FEA. *Open Engineering*, *10*(1), 769–775. https://doi.org/10.1515/eng-2020-0087
[37] Pimenta, A. R., Tavares, S. S. M., Dias, D. F., Correa, S. R., Sobreiro, A. L., & Diniz, M. G. (2021). Failure analysis of a titanium hip prosthesis. *Journal of Failure Analysis and Prevention*, *21*(1), 28–35. https://doi.org/10.1007/s11668-020-01041-2
[38] Total Materia. (2024, October 9). Titanium and Titanium Alloys. Retrieved from https://www.totalmateria.com/en-us/articles/titanium-and-titanium-alloys/
[39] Total Materia. (2024). ASTM F75 CoCr Alloy Properties. Retrieved from https://www.totalmateria.com/en-us/material/3258457
[40] Total Materia. (2024). MP35N Properties. Retrieved from https://www.totalmateria.com/en-us/material/3309632
[41] ANSYS 2019. (2019). Engineering Simulation and 3D Design Software. Houston, PA, USA: Ansys Inc.
[42] Ashvith, K., Damodaran, B. K., Khan, M. D. A., & Alam, N. (2024). Finite element analysis of hip implants-review. In *AIP Conference Proceedings* (Vol. 3042, p. 020038). https://doi.org/10.1063/5.0198508
[43] Kaya, F., İnce, G., Avcar, M., & Yünlü, L. (2021). Kalça protezi tasariminin sonlu elemanlar yöntemi ile statik analizi. *Mühendislik Bilimleri ve Tasarım Dergisi*, *9*(1), 199–208. https://doi.org/10.21923/jesd.839995
[44] Cho, J.-U., & Lee, E.-J. (2004). A study on fatigue fracture under non-constant load. *Journal of the Korean Society of Industry-Academic Technology*, *5*(4), 286–291.
[45] Bader, Q., & Njim, E. (2014). Mean stress correction effects on the fatigue life behavior of steel alloys by using stress life approach theories. *International Journal of Emerging Technologies in Learning (iJET)*, *14*.
[46] Aghili, S. A., Hassani, K., & Nikkhoo, M. (2021). A finite element study of fatigue load effects on total hip joint prosthesis. *Computer Methods in Biomechanics and Biomedical Engineering*, *24*(14), 1545–1551. https://doi.org/10.1080/10255842.2021.1900133
[47] Kayabasi, O., & Ekici, B. (2007). The effects of static, dynamic and fatigue behavior on three-dimensional shape optimization of hip prosthesis by finite element method. *Materials & Design*, *28*(8), 2269–2277. https://doi.org/10.1016/j.matdes.2006.08.012
[48] Wimalasiri, D. H. R. J. (2009, January 1). *Enhancement of the fatigue performance of Ti-6Al-4V implant products*. *Ph.D. Thesis*. Sheffield Hallam University, United Kingdom. Retrieved from https://ui.adsabs.harvard.edu/abs/2009PhDT.....211W
[49] Munteanu, S., Munteanu, D., Gheorghiu, B., Bedo, T., Gabor, C., Cremascoli, P., … Pop, M. A. (2019). Additively manufactured femoral stem topology optimization: case study. *Materials Today: Proceedings*, *19*, 1019–1025. https://doi.org/10.1016/j.matpr.2019.08.016
[50] Ghosh, S., Abanteriba, S., Wong, S., Brkljača, R., & Houshyar, S. (2019). Optimisation of grafted phosphorylcholine-based polymer on additively manufactured titanium substrate for hip arthroplasty. *Materials Science and Engineering: C*, *101*, 696–706. https://doi.org/10.1016/j.msec.2019.04.017
[51] Campioni, I., Notarangelo, G., Andreaus, U., Ventura, A., & Giacomozzi, C. (2013). Hip Prostheses Computational Modeling: FEM Simulations Integrated with Fatigue Mechanical Tests. In U. Andreaus & D. Iacoviello (Eds.), *Biomedical Imaging and Computational Modeling in Biomechanics* (pp. 81–108). Dordrecht: Springer Netherlands. https://doi.org/10.1007/978-94-007-4270-3_5

[52] Delikanli, Y. E., & Kayacan, M. C. (2019). Design, manufacture, and fatigue analysis of lightweight hip implants. *Journal of Applied Biomaterials & Functional Materials*, *17*(2), 2280800019836830. https://doi.org/10.1177/2280800019836830

[53] He, Y., Burkhalter, D., Durocher, D., & Gilbert, J. M. (2018). Solid-Lattice Hip Prosthesis Design: Applying Topology and Lattice Optimization to Reduce Stress Shielding from Hip Implants. Presented at the 2018 Design of Medical Devices Conference, American Society of Mechanical Engineers Digital Collection. https://doi.org/10.1115/DMD2018-6804

[54] Joshi, T., Sharma, R., Kumar Mittal, V., & Gupta, V. (2021). Comparative investigation and analysis of hip prosthesis for different bio-compatible alloys. *Materials Today: Proceedings*, *43*, 105–111. https://doi.org/10.1016/j.matpr.2020.11.222

[55] Joshi, T., Sharma, R., Mittal, V. K., Gupta, V., & Krishan, G. (2022). Dynamic analysis of hip prosthesis using different biocompatible alloys. *ASME Open Journal of Engineering*, *1*(011001). https://doi.org/10.1115/1.4053417

[56] Hosseini, S. (2012). Fatigue of Ti-6Al-4V. In *Biomedical Engineering - Technical Applications in Medicine*. IntechOpen. https://doi.org/10.5772/45753